**RESEARCH LETTER**

# Role of the eastern boundary-generated waves on the termination of 1997 Indian Ocean Dipole event

Iskhaq Iskandar[1*], Motoki Nagura[2] and Michael J. McPhaden[3]

## Abstract

The termination of Indian Ocean Dipole (IOD) events is examined in terms of equatorial wave dynamics. In situ and satellite observations combined with an output from a linear wave model are used in this study. Our emphasis is on the 1997 IOD event but our results apply to other positive IOD events as well. We find that the termination of anomalously cold sea surface temperature (SST) in the eastern pole of the dipole is associated with a warming tendency caused by the net surface heat fluxes. However, net surface heat fluxes alone cannot explain the total change in the SST. We show that during the peak phase of an IOD event, the weakening of zonal heat advection caused by eastern boundary-generated Rossby waves combined with the reduction of vertical entrainment and diffusion creates favorable conditions for surface heat fluxes to warm the SST in the eastern basin.

**Keywords:** Indian Ocean Dipole, Kelvin waves, Reflected Rossby waves, Zonal heat advection

## Key Points

1. Zonal heat advection significantly weakens during the termination phase of theIOD.
2. Weakening of zonal heat advection is due to eastern boundary-generatedRossby waves.
3. Net surface heating more effectively warms the SST as this advective cooling tendency weakens.

## Introduction

The Indian Ocean Dipole (IOD) is a coupled ocean–atmosphere phenomenon in the tropical Indian Ocean (Saji et al. 1999; Webster et al. 1999; Murtugudde et al. 2000). A zonal sea surface temperature (SST) gradient with negative SST anomalies (SSTA) off Java-Sumatra and positive SSTA in the central/western tropical Indian Ocean characterizes a positive IOD event. The IOD follows a seasonal pattern, beginning in the boreal spring and early summer, peaking in the fall, and ending the following winter (Saji et al. 1999). There is a negative phase to the IOD that evolves along a similar time line with oppositely signed anomalies, though of generally weaker amplitude.

The evolution of IOD events is associated with the suppression of convection over the eastern equatorial Indian Ocean and the enhancement of convection over the western equatorial Indian Ocean. This westward movement of the convection zone results in rainfall deficits in Indonesia and Australia, and excess rainfall in east Africa, India, and parts of South Asia (Ashok et al. 2003; Yamagata et al. 2004; Meyers et al. 2007). Furthermore, IOD episodes can influence global climate via atmospheric teleconnections (Saji and Yamagata 2003).

Ocean dynamics, notably equatorial Kelvin wave and Rossby wave excitation and propagation, play a significant role in the evolution of IOD events (Saji et al. 1999; Webster et al. 1999; Vinayachandran et al. 1999;

*Correspondence: iskhaq@mipa.unsri.ac.id
[1] Department of Physics, Faculty of Mathematics and Natural Sciences, University of Sriwijaya, Jl. Palembang—Prabumulih, Km. 32, Indralaya, Ogan Ilir (OI), Indralaya, Sumatra Selatan 30662, Indonesia
Full list of author information is available at the end of the article

Iskandar *et al. Geoscience Letters*     (2021) 8:35

Page 2 of 7

Murtugudde et al. 2000). During the development phase of a positive IOD event, upwelling equatorial Kelvin waves generated by easterly wind anomalies elevate the thermocline in the eastern equatorial Indian Ocean and depress it in the western basin. The shoaling of the thermocline in the eastern basin is further strengthened by anomalously strong local upwelling off Sumatra and Java owing to a strengthening of southeasterly wind anomalies along the coast. Meanwhile, in the southwestern equatorial Indian Ocean, downwelling Rossby waves generated in the season preceding the peak of an IOD event cause a deeper thermocline and warm SSTs there (Chambers et al. 1999; Vinayachandran et al. 1999; Rao et al. 2002; Feng and Meyers 2003; McPhaden and Nagura 2014).

Several mechanisms have been proposed for the termination of the IOD events. Murtugudde et al. (2000) hypothesized that the net-surface heat flux played a major role in SSTA warming in the eastern pole during the termination of the 1997 IOD event. A similar mechanism has been proposed for the termination of the 2006 IOD event (Horii et al. 2008). Furthermore, Li et al. (2002) proposed that solar and latent heat fluxes contribute primarily to SSTA warming near the eastern pole, with zonal advection providing a secondary contribution. Tokinaga and Tanimoto (2004) suggested that seasonal shifts in monsoonal winds during boreal autumn–winter reduced latent heat losses, resulting eradicating cold SSTA in the eastern equatorial Indian Ocean.

Oceanic equatorial waves have also been argued to play an important role in the termination of the IOD events (Rao and Yamagata 2004; Yuan and Liu 2009; McPhaden and Nagura 2014). Rao and Yamagata (2004) noted the appearance enhanced intraseasonal variability in the equatorial westerly winds prior to the termination of most IOD events. They argued that these westerlies generated anomalously strong downwelling equatorial Kelvin waves to terminate IOD events by deepening the thermocline and warming SST in the eastern basin. Meanwhile, Yuan and Liu (2009) attributed the termination of the IOD events to downwelling equatorial and off-equatorial Rossby waves reflecting at the western boundary into downwelling equatorial Kelvin waves, which subsequently propagate eastward to deepen thermocline and warm SST in the eastern equatorial Indian Ocean. McPhaden and Nagura (2014) also noted the importance of equatorial Rossby to Kelvin wave energy conversion at the western boundary in their analysis of IOD variability.

Previous studies have evaluated the mixed layer heat budget in the eastern equatorial Indian Ocean associated with the termination of IOD events (Murtugudde et al. 2000; Du et al. 2008; Chen et al., 2016). Murtugudde et al. (2000) have suggested that the termination of strong positive IOD event by the end of 1997 was associated with the SST warming due to a weakening of alongshore and equatorial winds, resulting in reduced latent heat loss and a shallow mixed layer. Du et al. (2008) have suggested that the thermocline plays a prominent role in generating and maintaining SSTA during the positive IOD years. Moreover, they proposed that the surface heat flux primarily caused the SST warming at the end of the IOD event. Furthermore, Chen et al. (2016) also noted that SST warming in the eastern equatorial Indian Ocean during the termination period of the positive IOD event in boreal winter was predominantly controlled by the surface heat flux, though the contribution from horizontal advection was not negligible.

Interestingly, Nagura and McPhaden (2010a) demonstrated that zonal currents along the equator lead zonal wind stress during the decay phase of the IOD. This phasing between currents and winds is a consequence of eastern-boundary-generated Rossby waves that reverse the zonal currents earlier than the zonal wind stress. These results suggest a possible role for the eastern-boundary-generated Rossby waves in the termination of the IOD events.

The objective of this study, therefore, is to quantitatively evaluate the role of eastern-boundary-generated Rossby waves on the termination of the IOD events. In situ and satellite observations are used to evaluate the thermodynamics of the IOD events, while outputs from a wind-driven, linear, continuously stratified long-wave ocean model are used to examine the dynamics of the IOD events. We will focus only on positive events and generally use the term IOD rather than positive IOD to refer to them, recognizing that negative events occur as well. We will return to the issue of asymmetries between positive and negative IOD events in the final section.

## Data and model

Surface current data are taken from the Ocean Surface Current Analysis-Realtime (OSCAR) (Bonjean and Lagerloef 2002). These current data are calculated based on a simplified ocean mixed layer model, assuming quasi-steady wind-driven and geostrophic flow dynamics. Satellite SSH, SST and surface wind data are used in the model to constrain the geostrophic and ageostrophic components of flow. This study used a 5 days, $1 \times 1$ gridded OSCAR data from 21 October 1992 to 1 September 2010.

We also use daily surface winds from the European Centre for Medium-Range Weather Forecasts (ECMWF) ERA-Interim for a period of January 1990 to December 2009 (Dee et al. 2011). In addition, SST time series derived from NOAA-Optimum Interpolation Sea Surface Temperature Analysis (OI-SST Ver. 2) are also used (Reynolds et al. 2002). Weekly SST products on $1 \times 1$

grid from January 1993 to December 2009 are used in the present study. Daily TropFlux surface heat fluxes (Kumar et al. 2011) from January 1989 to December 2009 are also used. This data set is available on $1 \times 1$ grid. Note that anomalies for all variables are calculated with respect to mean climatology from January 1993 to December 2008, when all data sets are available.

The model utilized in this study is a continuously stratified linear long-wave model on an equatorial β plane, similar to that used in Nagura and McPhaden (2010a, 2010b, 2012). The model uses the first ten baroclinic modes and 15 meridional modes for both Kelvin and Rossby waves. It encompasses the tropical Indian Ocean region from 40°E to 100°E and is bordered on the east and west by a meridional wall. The model is forced with daily wind stress for a period of 1 January 1980–30 April 2010. Previous studies have shown that this simple model well simulated observed sea level and zonal current variabilities in the equatorial Indian Ocean (Nagura and McPhaden 2010a, 2010b, 2012). However, the model simulated zonal currents sometimes differ from the observed results. This discrepancy could be due to nonlinear terms neglected in the simple model, errors in the winds employed as the model forcing, and/or errors in the OSCAR current product (Nagura and McPhaden 2010b).

## Results

Figure 1b illustrates the time series of the dipole mode index (DMI) from January 1993 to December 2009, which is defined as SSTA differences between the western and eastern equatorial Indian Ocean (Saji et al. 1999). There were three major IOD events during this time, namely, in 1994, 1997 and 2006 when the DMI was about twice its standard deviation. In addition, we also observed three weak positive IOD events in 2003, 2007 and 2008. The time series also shows two significant negative IOD events in 1996 and 1998. These events are consistent with those identified by the Bureau of Meteorology of Australia (http://www.bom.gov.au/climate/iod/). In this study, we focus on the termination of positive IOD events, with emphasis on the strongest of these in 1997.

The contribution of horizontal heat advection to the termination of IOD event was quantified in terms of the mixed layer temperature balance defined as (Vialard et al. 2008)

$$\frac{\partial T}{\partial t} = \frac{Q + q}{\rho C h} - u \frac{\partial T}{\partial x} - v \frac{\partial T}{\partial y} + R, \qquad (1)$$

where $T$ is mixed layer temperature, which we will use as a proxy for SST (Horii et al. 2013). In Eq. (1), $t$ indicates time, while $x$ and 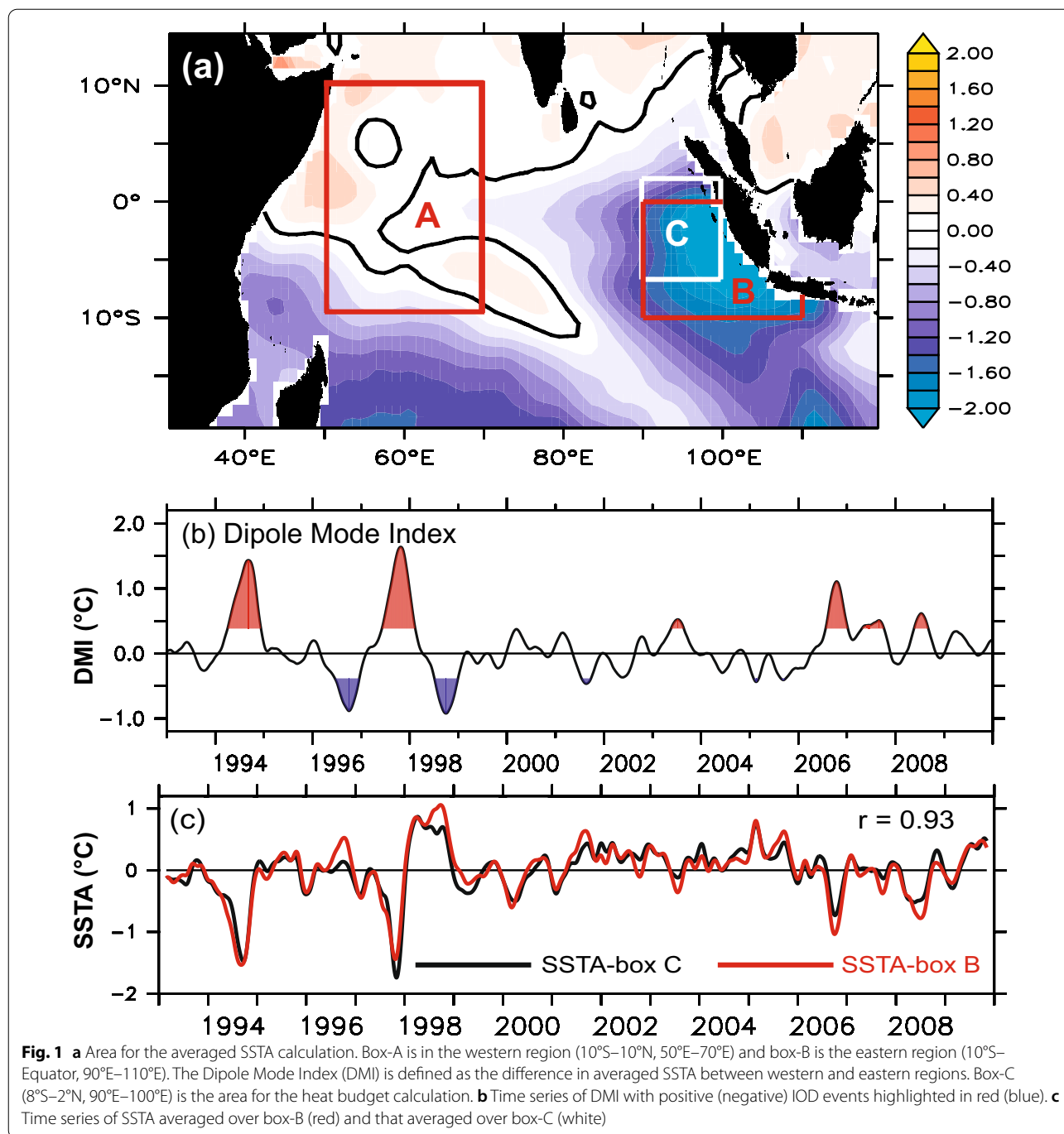$y$ denote the zonal and meridional direction, respectively. $\rho$ is the density of seawater (1026 kg m$^{-3}$), $C$ is the specific heat capacity of seawater (3986 J kg$^{-1}$ K$^{-1}$), $h$ is the depth of mixed layer, and $u$ and $v$ are the zonal and meridional velocity averaged over the mixed layer, respectively. $Q$ is the net surface heat flux and $q$ is the downward shortwave radiation at the bottom of the mixed layer. The later is estimated as $q = -0.47 \, Q_{sw} \, e^{(-0.04 \, h)}$, where $Q_{sw}$ indicate the shortwave radiation on the ocean surface (Wang and McPhaden 1999). The last term in Eq. (1) is the residual ($R$), which consists of physical processes that cannot be explicitly calculated, namely, a combination of horizontal and vertical diffusion and vertical entrainment at the bottom of the mixed layer. The residual also contains computational errors associated with terms that are explicitly estimated. However, we assume that these computational errors are small and interpret the residual in terms of the neglected physical processes, especially associated with vertical turbulent entrainment and diffusion as is commonly done (e.g., McPhaden 1982; Vialard et al. 2008).

Subsurface temperature and salinity data from Argo observations from January 2005 to December 2009 were used to calculate the monthly mixed layer depth ($h$). Considering the effect of salinity on the stratification in the eastern equatorial Indian Ocean, we estimate the mixed layer depth as a depth at which the density is 0.2 kg m$^{-3}$ larger than the surface density (Kumar et al. 2011). Since there is no observed temperature and salinity data for the period from January 1993 to December 2004, we used the mean climatology of the mixed layer based on the time series over the period of January 2005–December 2009.

The mixed layer temperature balance was calculated for a region in the eastern equatorial Indian Ocean between 8°S–2°N and 90°E–100°E (Fig. 1a). SSTA in this region is highly correlated with SSTA in the eastern pole of the IOD ($r = 0.93$ which is significantly nonzero with 95% confidence) for the period of January 1993–December 2009 (Fig. 1c) and so is representative of variability in the eastern pole of the dipole. It has the advantage though of being away from the irregular eastern boundary and in the equatorial waveguide, where wave processes can be readily diagnosed with the linear wave model.
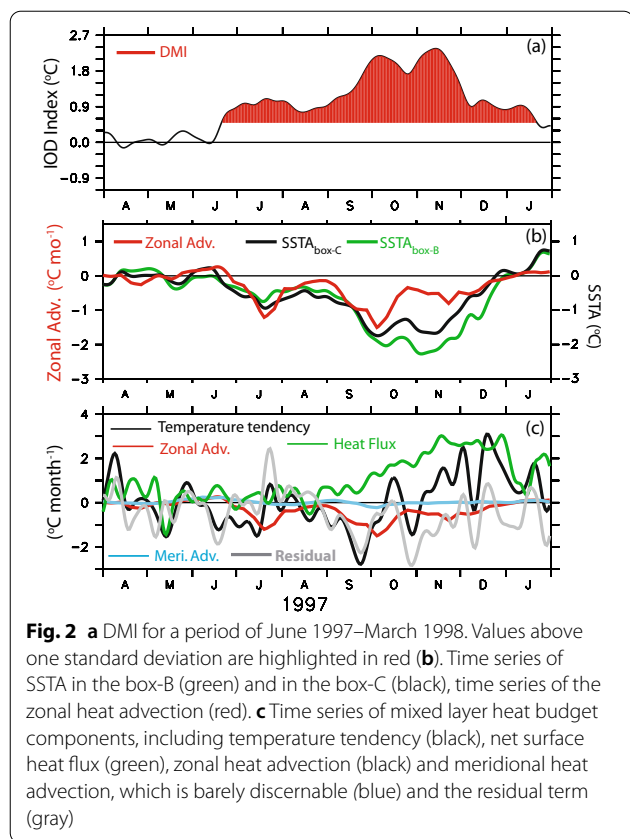
Horizontal advection is calculated based on the formula proposed by Lee et al. (2004) in terms of heat fluxes across each interface of the designated domain relative to a reference temperature. Here, we used a spatially averaged SST over the region between 8°S–2°N and 90°E–100°E (Fig. 1a) as the reference temperature.

We start by examining the evolution of the Dipole Mode Index (DMI) associated with the IOD event in 1997. A positive DMI started to develop in mid-June corresponding to SST cooling in the eastern pole of the IOD (Fig. 2a, b). In September, a rapid increase of the DMI

**Fig. 1** **a** Area for the averaged SSTA calculation. Box-A is in the western region (10°S–10°N, 50°E–70°E) and box-B is the eastern region (10°S–Equator, 90°E–110°E). The Dipole Mode Index (DMI) is defined as the difference in averaged SSTA between western and eastern regions. Box-C (8°S–2°N, 90°E–100°E) is the area for the heat budget calculation. **b** Time series of DMI with positive (negative) IOD events highlighted in red (blue). **c** Time series of SSTA averaged over box-B (red) and that averaged over box-C (white)

coincided with a rapid SST cooling event in the eastern Indian Ocean that began towards the end of August and continued until mid-November. There were two negative SST maxima in the eastern pole of the IOD occurring in early October and mid-November (Fig. 2a). We note that the onset of SST cooling in September corresponds well with zonal heat advection that shows an anomalous cooling from early September through early October,

suggesting the critical role of zonal heat advection in the development of the IOD event (Fig. 2a, b). Furthermore, the inferred vertical entrainment and diffusion across the base of the mixed layer exhibits a cooling tendency at about the same time as SST begins to cool (Fig. 2c). The termination of the IOD is identified by a rapid decrease of the DMI from mid-November to early December before it completely returns to normal condition in mid-January
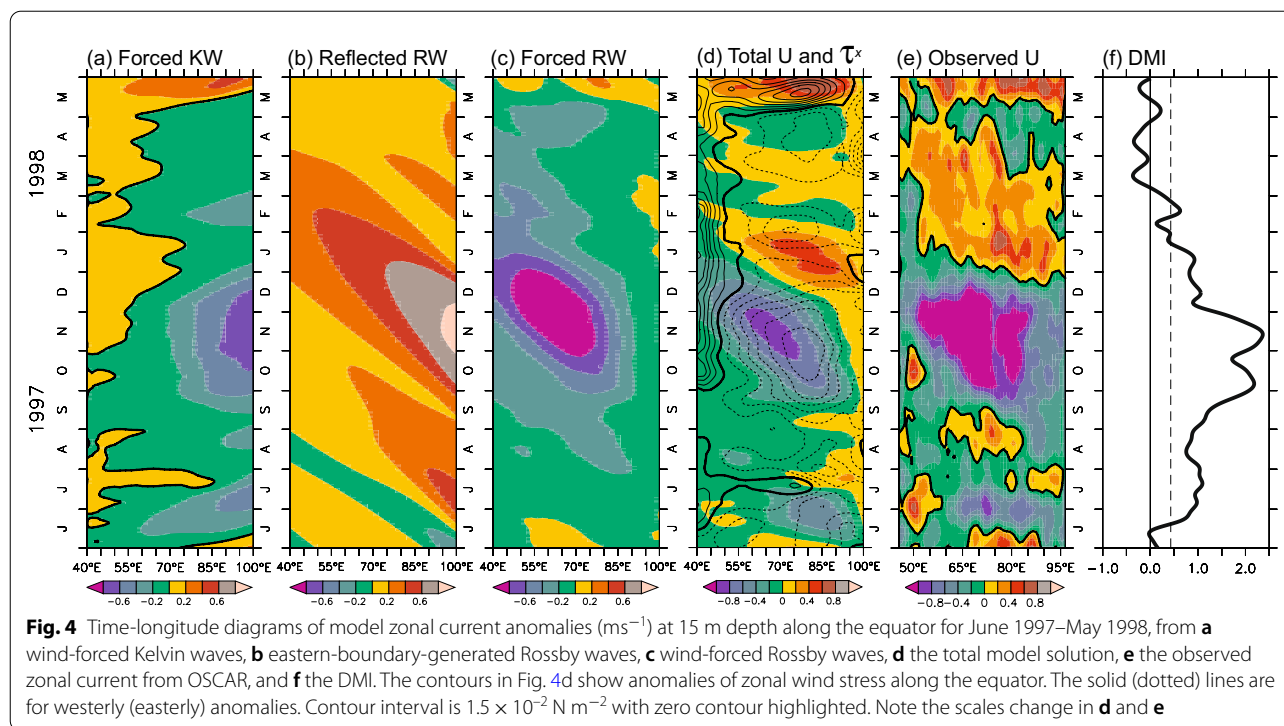
Iskandar *et al. Geoscience Letters*     (2021) 8:35

Page 5 of 7



**Fig. 2** **a** DMI for a period of June 1997–March 1998. Values above one standard deviation are highlighted in red (**b**). Time series of SSTA in the box-B (green) and in the box-C (black), time series of the zonal heat advection (red). **c** Time series of mixed layer heat budget components, including temperature tendency (black), net surface heat flux (green), zonal heat advection (black) and meridional heat advection, which is barely discernable *(*blue) and the residual term (gray)



**Fig. 3** Time series of **a** zonal current anomaly at box-C for June 1997–March 1998 from the OSCAR (black-dashed), the total model solution (black), eastern-boundary-generated Rossby waves (green), and the wind-forced Kelvin wave (red), **b** zonal wind stress at 90 °E (black) and that at 80 °E (red)

1998 (Fig. 2a). Interestingly, the timing of DMI decrease and the SST warming tendency in the eastern pole during October is associated with the weakening of vertical entrainment as well as zonal heat advection (Fig. 2c).

We next examine the relative role of different terms in the mixed layer temperature balance (Fig. 2c). We can see that during the development of the IOD event in September, the cooling tendency was associated with westward (negative) zonal heat advection linked to anomalous westward currents driven by easterly wind anomalies (Fig. 3a, b). In addition, vertical processes also tend to cool (Fig. 2c) consistent with earlier studies that noted anomalously strong upwelling-mediated entrainment and turbulent mixing generated cold SSTs in the eastern pole of the IOD during positive events (Murtugudde et al. 2000; Du et al. 2008). Later, during the termination of the event, net surface heat flux plays a role in SST warming. However, there is a phase lag between the net surface heat flux variations and the weakening of warming tendency. In particular, net surface heat flux leads the surface warming by about 1 month. Interestingly, there was abrupt SST warming and DMI decrease during October, which is associated with a weakening of both zonal heat advection and vertical entrainment/diffusion (Fig. 2c). From November toward the end of the
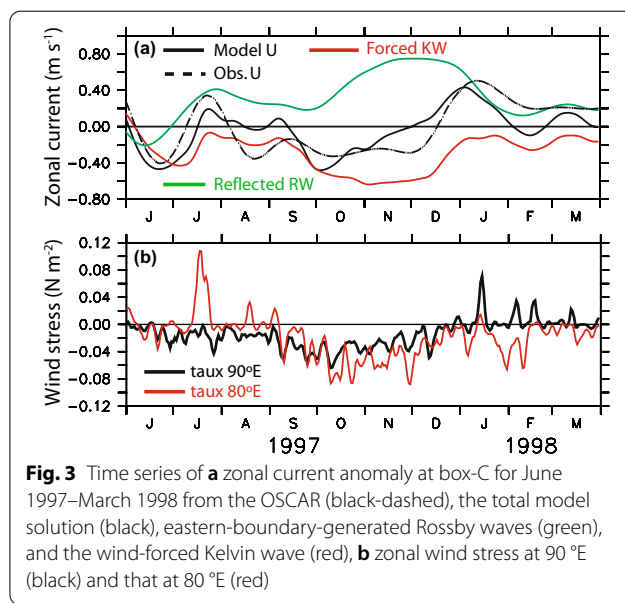
event in December, the surface heat flux becomes effective at warming the surface layer after zonal heat advection and vertical processes diminish in intensity. Thus, the weakening of zonal heat advection and inferred vertical turbulent entrainment and diffusion provide conditions favorable for surface heat flux to warm SST during the termination of the IOD event. Note that meridional advection has little influence on the overall balance (Fig. 2c).

In order to examine the dynamics of the zonal current anomalies along the equator, we evaluate the results of our linear wave model (Fig. 4). The model simulates reasonably well the anomalous westward zonal currents during the peak phase of the IOD in October–November (Figs. 3a, 4d, e). It is shown that westward zonal currents in the eastern basin are mainly due to wind-forced Kelvin waves, while westward currents in the central and western basins are mainly due to Rossby waves (Fig. 4a, c). As previously noted by Nagura and McPhaden (2010a), zonal currents along the equator eventually become eastward in late November although the zonal winds continue to be westward (Fig. 4d). Our model clearly indicates that this reversal is mainly generated by eastern boundary-generated Rossby waves (Fig. 4b, d). The timing of this zonal current reversal during the termination of the IOD event in late November/early December coincides with the weakening of the zonal heat advection in mixed layer temperature analysis (Fig. 2c). The combination of Kelvin and Rossby waves to the total model zonal velocity along the equator in our target region of 8°S–2°N, 90°E–100°E (Fig. 3) highlights the central role of eastern-boundary-generated Rossby waves in the termination of the IOD

**Fig. 4** Time-longitude diagrams of model zonal current anomalies (ms$^{-1}$) at 15 m depth along the equator for June 1997–May 1998, from **a** wind-forced Kelvin waves, **b** eastern-boundary-generated Rossby waves, **c** wind-forced Rossby waves, **d** the total model solution, **e** the observed zonal current from OSCAR, and **f** the DMI. The contours in Fig. 4d show anomalies of zonal wind stress along the equator. The solid (dotted) lines are for westerly (easterly) anomalies. Contour interval is $1.5 \times 10^{-2}$ N m$^{-2}$ with zero contour highlighted. Note the scales change in **d** and **e**

event. Note that the contributions from the wind-forced Rossby and the reflected Kelvin waves in this region are negligible (not shown).

## Conclusions

In this study, we have examined the role of eastern boundary-generated Rossby waves on the termination of the IOD events, with emphasis on the strong 1997 IOD event. We used available observational data combined with output from a continuously stratified long equatorial wave model. The model allows us to diagnose separately the effects of wind-forced and boundary-generated waves on the zonal currents and how they affect the surface layer temperature balance.

Our analysis reveals that the termination of negative SSTAs in the eastern basin is associated with a warming tendency due to the net surface heat fluxes. However, the net surface heat fluxes alone cannot explain the total change in the mixed layer temperature. The heat budget analysis shows a phase mismatch between the evolution of the net surface heat fluxes and SST warming tendencies, indicating that other factors contribute to the termination of IOD events. Here we propose that a weakening of the cooling effects of zonal heat advection plays an important role in the termination of the IOD in addition to the weakening of vertical entrainment diffusion at the bottom of the mixed layer. As these cooling tendencies diminish, net surface heating can more effectively warm

SST. Moreover, the weakening of zonal heat advection is associated with a reversal of the zonal current anomalies along the equator, from westward to eastward. Our model indicates that this reversal is generated mainly by eastern boundary generated Rossby waves.

Though we have focused mainly on the 1997 event, we examined other positive IOD events (e.g., 1994 and 2006) and found that similar mechanisms were at work; in particular that zonal currents associated with eastern boundary generated Rossby lead to a reduction in cooling by zonal advection during the termination of each event. This situation is analogous to the role that eastern boundary-generated currents play in the termination of ENSO events as proposed in the advective-reflective oscillator theory of Picaut et al. (1997).

We have not addressed the role of oceanic equatorial waves on the mixed layer temperature balance during negative IOD events. Horii et al. (2013) described the asymmetry in the mixed layer temperature balance in the southeastern tropical Indian Ocean between positive and negative IOD events, and suggested that surface heat flux plays a dominant role in the mixed layer temperature balance during the evolution of the negative 2010 IOD event. Whether this result applies to all negative IOD events, or whether there is a possible role for zonal advection related to equatorial wave dynamics during the development and demise of negative IOD events, is an open question.

Iskandar *et al. Geoscience Letters*        (2021) 8:35

Page 7 of 7

## Declarations

**Competing interests**
The authors declare that they have no competing interests.

**Author details**
[1]Department of Physics, Faculty of Mathematics and Natural Sciences, University of Sriwijaya, Jl. Palembang—Prabumulih, Km. 32, Indralaya, Ogan Ilir (OI), Indralaya, Sumatra Selatan 30662, Indonesia. [2]Japan Agency for Marine-Earth Science and Technology, Yokosuka, Kanagawa, Japan. [3]Pacific Marine Environmental Laboratory, NOAA, Seattle, WA, USA.

## References

Ashok K, Guan Z, Yamagata T (2003) Influence of the Indian Ocean Dipole on the Australian winter rainfall. Geophys Res Lett 30(15):1821. https://doi.org/10.1029/2003GL017926

Bonjean F, Lagerloef GSE (2002) Diagnostic model and analysis of the surface currents in the tropical Pacific Ocean. J Phys Oceanogr 32:2938–2954

Chambers DP, Tapley BD, Stewart RH (1999) Amomalous warming in the Indian Ocean coincident with El Niño. J Geophys Res 104:3035–3047. https://doi.org/10.1029/1998JC900085

Chen W, Han Y, Li DW (2016) Interannual variability of equatorial eastern Indian Ocean upwelling: local versus remote forcing. J Phys Oceanogr 46:789–807. https://doi.org/10.1175/JPO-D-15-0117.1

Dee DP, Uppala SM, Simmons AJ et al (2011) The ERA-Interim reanalysis: configuration and performance of the data assimilation system. Q J R Meteorol Soc 137:553–597

Du Y, Qu T, Meyers G (2008) Interannual variability of sea surface temperature off Java and Sumatra in a global GCM. J Climate 21:2451–2465. https://doi.org/10.1175/2007JCLI1753.1

Feng M, Meyers G (2003) Interannual variability in the tropical Indian Ocean: a two-year time-scale of Indian Ocean Dipole. Deep-Sea Res 50:2263–2284

Horii T, Hase H, Ueki I, Masumoto Y (2008) Oceanic precondition and evolution of the 2006 Indian Ocean Dipole. Geophys Res Lett 35:L03607. https://doi.org/10.1029/2007GL032464

Horii T, Ueki I, Ando K, Mizuno K (2013) Eastern Indian Ocean warming associated with the negative Indian Ocean dipole: a case study of the 2010 event. J Geophys Res Oceans 118:536–549. https://doi.org/10.1002/jgrc.20071

Kumar BP, Vialard J, Lengaigne M, Murty VSN, McPhaden MJ (2011) TropFlux: air-sea fluxes for the global tropical oceans–description and evaluation against observations. Clim Dyn. https://doi.org/10.1007/s00382-011-1115-0

Lee T, Fukumori I, Tang B (2004) Temperature advection: internal versus external processes. J Phys, Oceanogr 34:1936–1944

Li T, Zhang Y, Lu E, Wang D (2002) Relative role of dynamic and thermodynamic processes in the development of the Indian Ocean dipole: an OGCM diagnosis. Geophys Res Lett 29(23):2110. https://doi.org/10.1029/2002GL05789

McPhaden MJ (1982) Variability in the central equatorial Indian Ocean, part II: oceanic heat and turbulent energy balance. J Mar Res 40:403–419

McPhaden MJ, Nagura M (2014) Indian Ocean dipole interpreted in terms of recharge oscillator theory. Clim Dyn 42(5–6):1569–1586

Meyers GA, McIntosh PC, Pigot L, Pook MJ (2007) The year of El Niño, La Niña, and interactions with the tropical Indian Ocean. J Clim 20:2872–2880

Murtugudde R, McCreary JP, Busalacchi AJ (2000) Oceanic processes associated with anomalous events in the Indian Ocean with relevance to 1997–98. J Geophys Res 105(C2):3295–3306

Nagura M, McPhaden MJ (2010a) The dynamics of zonal current variations associated with the Indian Ocean Dipole. J Geophys Res 115:C11026. https://doi.org/10.1029/2010JC006423

Nagura M, McPhaden MJ (2010b) Wyrtki jet dynamics: seasonal variability. J Geophys Res 115:C07009. https://doi.org/10.1029/2009JC005922

Nagura M, McPhaden MJ (2012) The dynamics of wind-driven intraseasonal variability in the equatorial Indian Ocean. J Geophys Res 115:C07009. https://doi.org/10.1029/2011JC007405

Picaut J, Masia F, du Penhoat Y (1997) An advective-reflective conceptual model for the oscillatory nature of the ENSO. Science 277:663–666

Rao SA, Yamagata T (2004) Abrupt termination of Indian Ocean dipole events in response to instraseasonal oscillations. Geophys Res Lett 31:L19306. https://doi.org/10.1029/2004GL020842

Rao SA, Behera SK, Masumoto Y, Yamagata T (2002) Interannual subsurface variability in the tropical Indian Ocean with a special emphasis on the Indian Ocean dipole. Deep Sea Res 49:1549–1572

Reynolds RW, Rayner NA, Smith TM, Stokes DC, Wang WQ (2002) An improved in situ and satellite SST analysis for climate. J Climate 15:1609–1625

Saji NH, Yamagata T (2003) Possible impacts of Indian Ocean Dipole mode events on global climate. Clim Res 25:151–169

Saji NH, Goswami BN, Vinayachandran PN, Yamagata T (1999) A dipole mode in the tropical Indian Ocean. Nature 410:360–363

Tokinaga H, Tanimoto Y (2004) Seasonal transition of SST anomalies in the tropical Indian ocean during El Nino and Indian Ocean dipole years. J Meteor Soc Japan 82:1007–1018

Vialard J, Foltz GR, McPhaden MJ, Duvel JP, de Boyer Montégut C (2008) Strong Indian Ocean sea surface temperature signals associated with the Madden-Julian Oscillation in late 2007 and early 2008. Geophys Res Lett 35:L19608. https://doi.org/10.1029/2008GL035238

Vinayachandran PN, Saji NH, Yamagata T (1999) Response of the equatorial Indian Ocean to an unusual wind event during 1994. Geophys Res Lett 26:1613–1616. https://doi.org/10.1029/1999GL900179

Wang W, McPhaden MJ (1999) The surface layer heat balance in the equatorial Pacific Ocean. Part I: mean seasonal cycle. J Phys Oceanogr 29:1812–1831

Webster PJ, Moore AW, Loschnigg JP, Leben RR (1999) Coupled ocean-atmosphere dynamics in the Indian Ocean during 1997–98. Nature 401:356–360

Yamagata T, Behera SK, Luo J-J, Masson S, Jury M, Rao SA (2004) Copled ocean-atmosphere variability in the tropical Indian Ocean. Earth Clim Ocean Atmos Interact Geophys Monogr 147:189–212

Yuan D, Liu H (2009) Long-wave dynamics of sea level variations during Indian Ocean Dipole events. J Phys Oceanogr 39:1115–1132

## Publisher's Note

Springer Nature remains neutral with regard to jurisdictional claims in published maps and institutional affiliations.